Controlling Interferences in Smart Building IoT Networks using Machine Learning

Lynggaard, Per

[Link to publication from Aalborg University](#)

Controlling Interferences in Smart Building IoT Networks using Machine Learning

Per Lynggaard

Center for Communication and Information Technologies Aalborg University Denmark
A. C. Meyers Vænge 15, 2450 Copenhagen SV, Denmark; E-mail: perlyn@es.aau.dk

Abstract

The coexistence of many IoT networks in smart buildings poses a major challenge because they interfere mutually. In most settings this results in a greedy approach where each IoT node optimizes its own performance parameters like increasing transmit-power, etc. However, this means that interference levels are increased, battery powers are wasted, and spectrum resources are exhausted in high dense settings. To control interference levels, share spectrum resources, and lower the overall power-consumptions this paper proposes a centralized control scheme which is based on a nonlinear cost function. This cost function is optimized by using machine learning in the form of a binary particle swarm optimization algorithm. It has been found that this approach shares the spectrum in a fair way, it saves power and lowers the interference levels, and it dynamically adapts to network changes.

Biographical note:

Per Lynggaard received his M.Sc. in EE and IT and his Ph.D. in the areas of artificial intelligence and Internet of Things (IoT) from Aalborg University, Denmark. Dr. Lynggaard is employed at Aalborg University as an associate professor with the following research and teaching areas: digital signal processing, machine learning, wireless communication, and Internet of Things. He has supervised numerous master and bachelor projects and lectured in several Ph.D. courses.

Introduction

The amount of traffic emanating from the indoor Internet of Things (IoT) in a 5G context brings many benefits and some major challenges (Lynggaard & Skouby, 2015). Especially, mutual interferences, energy consumptions, and (Quality of Service) QoS parameters are key challenges for IoT networks which call for a multi-objective optimization technique (Abdellaoui, et al., 2013), (Muhammad, et al., 2015). Mutual interferences among the IoT nodes limit the network QoS by increasing the amount of packet-congestions, reduce the Signal to Noise Ratios (SNR), and limits the overall spectral efficiency (Lynggaard & Skouby, 2015), (Chincoli & Liotta, 2018). Most IoT networks handle this problem by using a greedy approach where each IoT node optimizes its own performance-parameters such as bit-rate, energy consumption, and transmit-power (Lynggaard & Skouby, 2015). However, this approach increases the overall transmit-power, increases the energy consumption, and lowers the bit-rate for most nodes. Different approaches to deal with these challenges have been discussed in the literature. One approach implements a central controller that offers shared resource management to improve the QoS for all the IoT nodes in the same context (Yaacoub, 2016). A similar concept is proposed by Qiu et al. that optimizes the QoS for all the IoT nodes globally by using a fairness principle that leverages bit-rates, energy consumptions, and transmit-powers (Qiu & Chawla, 1999). It is noted that regulating the transmit-power adaptively for a multi-access wireless IoT sub-network is an effective means for increasing the spectral efficiency, reducing the power consumption, and increasing the energy efficiency (Weng, et al., 2014). Nevertheless, a key challenge for centralizing adaptive interference-control is the ability of the controllers to continuously track changes in the IoT networks and to adjust the transmit-power used by the individual IoT networks accordingly. These challenges have been addressed by

Chincoli et al. that used a machine learning approach based on "packet reception ratio" to update the transmit-power for all the nodes in a network (Chincoli & Liotta, 2018). A similar approach is followed by (Chincoli, et al., 2016) which uses the packet reception ratio to characterise the interference levels. Gogu et al. address the challenges by developing an algorithm which uses a "min-max fair link" scheme (Gogu, et al., 2014). An approach that uses particle swarm optimization for a fully connected cluster of IoTs has been proposed by Fré et al. (Fré, et al., 2015). They found that considerable energy savings can be obtained by controlling the transmit-power from a central controller. In addition, they concluded that the use of particle swarm optimization algorithm for optimizing the non-convex controller problem was a very efficient and resource limited method. Many similar approaches have been published as elaborated in a survey from Muhammad et al. (Muhammad, et al., 2015); However, there is a lack of research in approaches that use interference levels in combination with dynamically varying pathlosses, Rayleigh fading, and adjustable bit-rates to estimate the necessary transmit-power levels for the nodes in the system. A system based on this approach requires an efficient multi-objective nonconvex optimization scheme.

In this paper a central controller for smart buildings is presented, simulated, and elaborated. It calculates the transmit-power used in each apartment (sub-network) in a smart building based on initial estimated losses and feedbacks from the sub-networks in the form of their received SNR. The results from this calculation are sent to the sub-network Gateway Nodes (GWNs) which distribute these to their respective Wireless Internet of Things Nodes (WINs). The central controller uses a nonconvex cost-function to optimize the bit-rates of the sub-networks in a fair way and to minimize the amount of used power from the WINs. In order to solve this nonlinear cost-function a machine learning algorithm in the form of Binary Particle Swarm Optimization (BPSO) has been implemented. This algorithm has proven to be very effective in similar contexts to handle complex nonlinear problems (Fré, et al., 2015), (Kinhekar & Gupta, 2015), (Shi & Eberhart, 1999).

The method used in this paper is based on designing and constructing a simulation model which combines pathlosses, fading, transmit-power, and masking possibilities for some sensor node types with a powerful BPSO algorithm to provide and substantiate the potential of this approach. It is noted that only Rayleigh fading has been included in this work because it provides a worse case fading scenario compared to situations where line-of-sight is established, i.e. Rician fading takes place (Pathak & Katiyar, 2016), (Kumar, et al., 2013) . By using the simulation model, it has been found that the proposed approach is very effective, it provides a fair bit-rate allocation that is between 4 and 5 times fairer that a greedy approach, and it saves between 28 and 74 percent of the consumed energy compared to the greedy approach. This energy saving reduces the interference levels proportionally. Similarly, it has been found that the BPSO algorithm is very effective and efficient tool in this context.

BPSO

The Binary Particle Swarm Optimization (BPSO) algorithm is a specialization of the more generic Particle Swarm Optimization (PSO) algorithm family. This family is mostly used for optimization of nonconvex cost functions in a highly dimensional number space. Similar algorithms are: quasi-Newton BFGS, NEWUOA derivative free optimizer, Covariance Matrix Adaptation Evolution Strategy (CMA-ES), and the Differential Evolution (DE). A test performed by Auger et al. showed that the quasi-Newton BFGS and the NEWUOA algorithms perform well in case of separable quadratic functions; however, they show a strong decline in performance if the cost function becomes ill-conditioned (Auger†, et al., 2009). In contrast, the CMA-ES, DE, and PSO algorithms perform well even if the cost function becomes ill-conditioned; By using the principles of "Occam's razor" the PSO algorithm is chosen, because it is the simplest in terms of implementation complexity.

A mathematical description of the basic principles for the BPSO algorithm used in this work is presented in (1).

$$\bar{V}_i = \bar{V}_i(t-1) + \phi_1(\bar{P}_{i,best} - \bar{X}_i(t-1)) + \phi_2(\bar{G}_{best} - \bar{X}_i(t-1)) \qquad (1)$$

$$\bar{X}_i, \bar{P}_{i,best}, \bar{G}_{best} \in [b_0, b_1, ..., b_j], b \in \{0,1\}$$

$$\bar{V}_i \in [v_0, v_1, ..., v_j], v \in \{0, ..., 1\}, j \in \mathbb{Z}^*$$

$$s(\bar{V}_i) = \frac{1}{1 + e^{-\bar{V}_i}}$$

where ϕ_1 and ϕ_2 are positive random numbers from a uniform distribution. The velocity V_i is the probability that a bit in X_i will change in the next iteration. To quantise V a logistic function is used, i.e. if Sigmoid ($V_{i,j}$) is larger than ϕ_1 or ϕ_2 the corresponding bit j is changed in $X_{i,j}$ (Kennedy & Eberhart, 1997).

Many PSO based WSN algorithms have been derived. To set this work in perspective to these a short survey of the operating principles and the improvements of performance are presented in Figure 1 and Table 3. This survey is partly based on the work and principles used by Raghavendra et al. (Kulkarni & Venayagamoorthy, 2011).
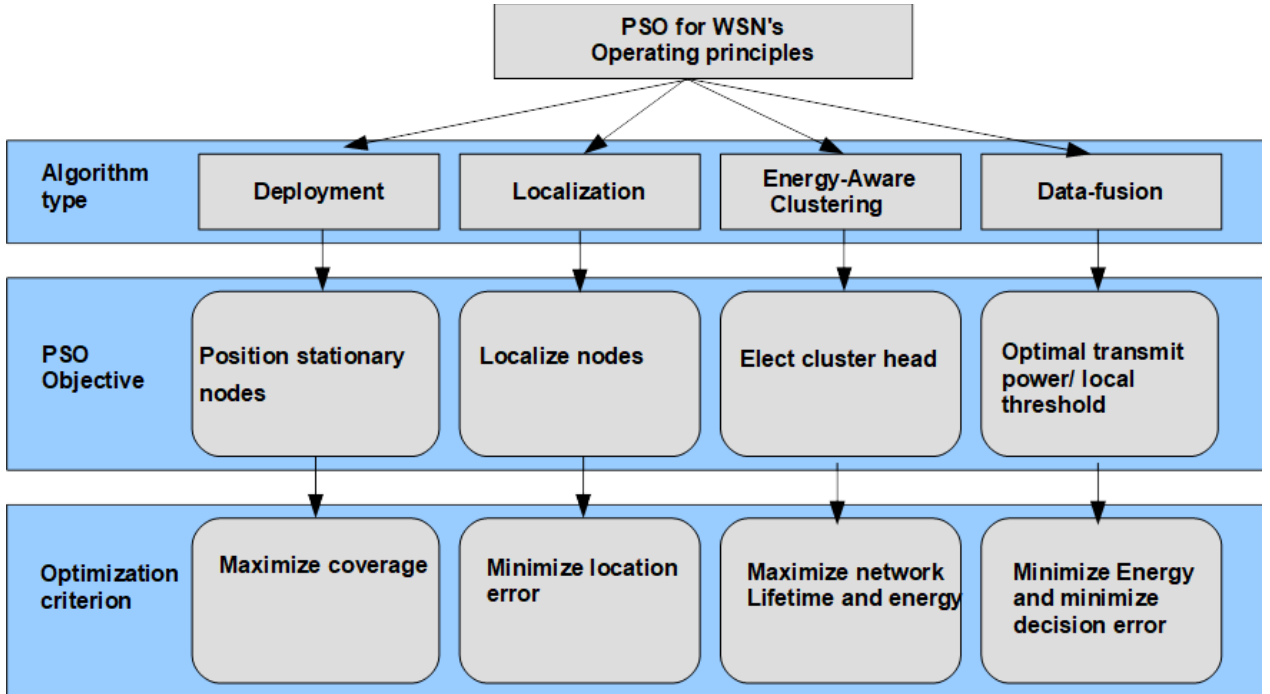

Figure 1, Survey of the operating principles used by different SPO types in relation to WSN.

Some of the key technical challenges in deploying and using WSN's are dynamic topology, ad-hoc spatial deployment- and constraints in resources such as bandwidth, energy supply, and computational power (Kulkarni & Venayagamoorthy, 2011). In order to deal with these challenges, they can be organized into the categories: node deployment, localization, energy-aware clustering, and data-aggregation. These categories are often formulated as nonlinear optimization problems with some given optimization criterions (Figure 1). To exemplify the optimization procedures often used in these categories selected works from different authors are provided in Table 1. It is noted that this is only a set of selected examples; nevertheless, a more in deep elaboration and many similar examples can be found in the work by Kulkarni et al. (Kulkarni & Venayagamoorthy, 2011).

Type	Algorithm type	Ref.	Performance discussion
Deployment	Particle Swarm	(Wang, et al., 2016)	Algorithm reaches a better network coverage

	Optimization with Coherent Velocity		(more than 90 percent) compared to ordinary algorithms.
Localization	PSO-ANN	(Gharghan, et al., 2016)	The PSO–ANN algorithm outperforms those based on the LNSM-based traditional method.
Energy-Aware Clustering	Improved PSO	(ZHOU, et al., 2017) Similar work: (Kuila & Jana, 2014)	Outperform many common algorithms such as: LEACH, TCAC, SEECH on parameters such as energy consumption and node-lifetime
Data-fusion	PECC-algoritme (PSO)	(Vimalarani, et al., 2015)	The algorithm improves performance in order to minimize the total consumed energy and increase the lifetime compared to similar WSN systems.

Table 1, Exemplification of optimization procedures used in selected works.

System Model

It his section the system model used in the simulation section is derived and elaborated.

System model overview

The system model covers a collection of apartments in a smart building where each apartment contains a GWN and some serving WINs, Figure 2. The IoT nodes in one apartment are wirelessly connected to the gateway node in that apartment only. Similarly, the gateway nodes from each apartment are connected via a wired network to a central controller located in the smart building. By using this concept, it is possible to regulate the interference levels and to enhance the QoS parameters such as bit-rate, packet loss, and delay for each WIN individually. In the absence of a central controller each GWC would optimize its own sub-network without considering the global interference level and the global power consumption.
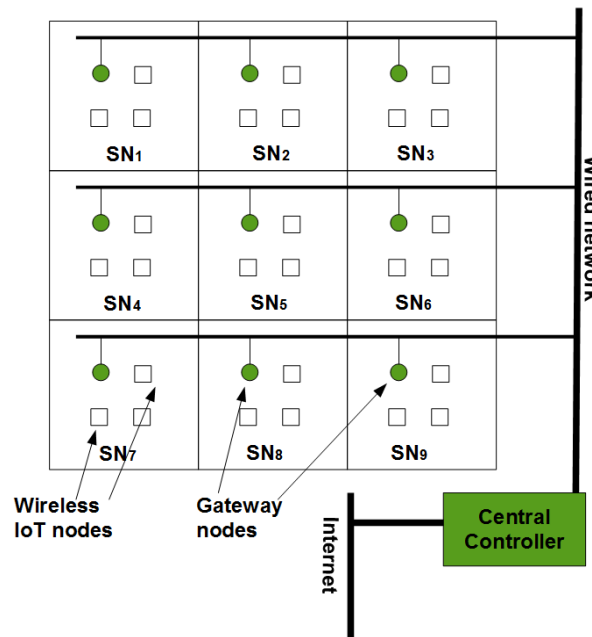

Figure 2, A model of a smart building with its apartments, IoT nodes, gateway nodes, and a central controller.

Ideally, such a system would work; however, in real-world settings, the spectrum available to the WINs is often limited to the ISM bands (ITU, 2018), which means that the GWN and WIN nodes must share the same spectrum. Many protocols are available for sharing spectrum in both the frequency and the time domains, but these are still limited by the laws of nature. One key problem is the interferences produced when many nodes use the same spectrum. In the settings illustrated in Figure 2 the spectrum used by a subsystem (a collection of a GWN node plus some WIN nodes) in one apartment potentially travels through walls, floors and roofs to the other apartments. Hence, when one of the WINs transmits to its

GWN it causes interferences to the other GWN nodes. However, the transmission from the GWNs to the WINs causes limited interferences only, because most of the traffic from the GWN is acknowledge-commands (ACK) and in some cases setting commands to actuators, etc.
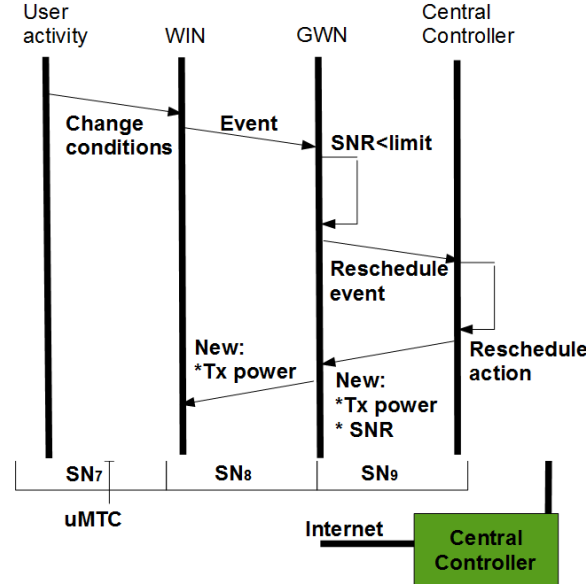

Figure 3, Sequence diagram with the steps performed when the model needs to be updated by the controller.

Most of the time the system is stationary, i.e. the interference levels and the bit-rate-fairness are maintained; however, if a disturbance is imposed (e.g. a user moves furniture, etc.) the system parameters change, and a re-run of the central controller is needed. This is activated by one or more of the GWNs which use their received averaged SNR to trigger this event, Figure 3.

Channel model

The primary factor in most channel-models is the path-loss (Λ), which can be calculated by using the modified ITU indoor model as (ITU, 2001) (2):

$$\Lambda_{dB} = 20\log_{10}(f) + N\log_{10}(d) + Pf(n) + Pw(q) - 28 \tag{2}$$

In this equation f is the frequency (MHz), N is the distance-loos-coefficient, $Pf()$ is the floor loss penetration factor, $Pw()$ is the wall penetration factor, q is the number of walls, and n is the number of floors. By considering the losses from fading fluctuations (2) can be written as (3):

$$\mathrm{E}_{dB} = \Lambda_{dB} + \chi + 10\log_{10}(\Delta(t)) \tag{3}$$

where X is the log-normal distributed shadowing effect with zero-mean and a standard deviation of σ and Δ is the contribution from Rayleigh fading, where it is assumed that the channels between the WINs and a GWN are stationary and have time-varying gains. The Rayleigh distribution assumes the impulse responses of the interference-channels are Gaussian distributed, which is true according to the central limit theorem in high density networks. The envelope of the channel response can be modelled by random variables having the following Probability Density Function (PDF) (Falahati, et al., 2003), (4):

$$p(\gamma) = \frac{1}{\Gamma} e^{-(\frac{\gamma}{\Gamma})} \tag{4}$$

where $p(\gamma)$ is the PDF and Γ is average received SNR. Similarly, the upper bound for the Bit Error Rate (BER) can be found as an approximation if it assumed that the nodes uses low order QAM such as BPSK (5) (Chung & Goldsmith, 2001):

$$BER \leq k_1 e^{(-\frac{k_2\gamma}{\zeta-1})} \ or \ \zeta \leq 1 - \frac{k_2\gamma}{\ln(\frac{BER}{k_1})} \tag{5}$$

In this equation k_1 is 0.2 and k_2 is 2, and ζ is the number of constellation points in the QAM signal, which in this work is considered a continuous variable. However, without loss of generality, this can be converted into discrete constellation points. By rewriting this equation in a form where $\log_2(\zeta)$ is on the left side and the upper bound is used - the similarity with the Shannon channel capacity theorem is notable (Sklar, 2002), (6):

$$\log_2(\zeta) = \log_2(1 - \frac{k_2\gamma}{\ln(\frac{BER}{k_1})}) = \log_2(1 + c_1\gamma) \tag{6}$$

$$\Psi(\gamma) = \frac{C(\gamma)}{B} = \log_2(\zeta) = \log_2(1 + c_1\gamma)$$

$$c_1 = -\frac{k_2}{\ln(\frac{BER}{k_1})}$$

Where C is the Shannon channel capacity and B is the bandwidth for the channel, similarly the C/B is the spectral efficiency with the dimension bits/seconds/Hz.

By combining (4) and (6) the average spectral efficiency for a channel with flat fading can be derived as (7):

$$\tilde{\Psi}(\gamma) = \int_0^{+\infty} \log_2(1 + c_1\gamma)p(\gamma)d\gamma \tag{7}$$

$$= \frac{1}{\ln(2)} \left(\left[-\ln(1 + c_1\gamma)e^{-\frac{\gamma}{\Gamma}} \right]_0^{+\infty} + \int_0^{+\infty} \frac{c_1}{1 + c_1\gamma} e^{-\frac{\gamma}{\Gamma}} d\gamma \right)$$

$$= \frac{1}{\ln(2)} \left(\int_0^{+\infty} \frac{c_1}{1 + c_1\gamma} e^{-\frac{\gamma}{\Gamma}} d\gamma \right)$$

$$= \frac{-e^{\frac{1}{c_1\Gamma}}}{\ln(2)} Ei(-\frac{1}{c_1\Gamma})$$

The first step uses the integration by parts theorem and the second step handles the divergent integral by considering its asymptotic limit. Finally, the result is derived as a function that uses the exponential integral $Ei()$.

Data-rates

The obtainable average data-rates in the channel between the WINs and the GWNs can be found by multiplying the average spectral efficiency $\Psi(\gamma)$ with the used bandwidth where it is noted that for QAM the spectral bandwidth is often equal to the symbol rate, i.e. the bandwidth excess-factor is close to one. Similarly, the SNR for a GWN can be found by dividing the received Rayleigh weighted signal with the sum of the interferences and the Gaussian distributed noise power in the channel. It is noted that the interferences from the other nodes (the nodes that do not participate in the communication) are considered as random noise in alignment with Arnab et al. (Nandi & Kundu, 2010). To elaborate the interferences some matrixes and vectors are defined (all vectors are column vectors):

The first matrix L contains the path-losses (2) and (3) (where the Rayleigh part in (3) is given by (4)) between the sub-network centres (SNk in Figure 2 where k is 1,2,..,9). Without loss of generality, this approximation assumes that the sub-network centres represent the position of the WGN and the transmitting WIN (8):

$$\widehat{L} = \begin{Bmatrix} l_{1,1} & ... & l_{1,I} \\ ... & l_{i,j} & ... \\ l_{I,1} & ... & l_{I,I} \end{Bmatrix} \quad i,j \in \{1,2,...,I\} \tag{8}$$

In this equation I is the number of sub-networks.

The second matrix contains a binary mask (m) which enables or disables the interferences that should be taken into account for each sub-network SN$_i$ where $i=\{1,2,...,I\}$ (9):

$$\widehat{M} = \begin{Bmatrix} m_{1,1} & ... & m_{1,I} \\ ... & m_{i,j} & ... \\ m_{I,1} & ... & m_{I,I} \end{Bmatrix} \quad \begin{matrix} i \in \{1,2,...,I\} \\ m \in \{0,1\} \end{matrix} \tag{9}$$

A transmit-power-vector is defined for each of the sub-networks as follows (10):

$$\overline{P}_{SN,i} = [P_1, P_2,..., P_I] \quad i \in \{1,2,...,I\} \tag{10}$$

Similarly, the path-loss between a WGN and a transmitting WIN in the same sub-network is defined as (11):

$$\overline{L}_{SN,i} = [L_1, L_2,..., L_I] \quad i \in \{1,2,...,I\} \tag{11}$$

By combining the path-loss matrix (L), the mask matrix (M), the transmit-power vector, and the path-loss inside a sub-network the SNR (γ) for each sub-network can be found (12):

$$\gamma = (\overline{P}_{SN} \circ \overline{L}_{SN}) \circ ((\widehat{L} \circ \widehat{M} \circ \widehat{E})^T \overline{P}_{SN})^{\circ -1} \tag{12}$$

$$\widehat{E}_{I \times I} = (a_{i,j}), \begin{cases} a_{i,j} = 0, \text{if } i = j \\ a_{i,j} = 1, \text{else} \end{cases}$$

where E is a hollow matrix, o is the Hadamard product operator, and o- is the Hadamard inverse matrix operator.

Utility maximisation

To maximize the utility of all the sub-networks in a smart building a QoS fairness-principle is deployed, which ensures that all the sub-networks have approximately the same bit-rates (v). With U$_i$ denoting a (GWN, WIN) pair in the i'th sub-network the objective is to maximize the overall bitrates (13):

$$\max_{\chi i} U_{tot} = \sum_{i=1}^{I} U_i \qquad (13)$$

Subject to:

$$\xi_1 \leq \frac{\upsilon_i}{\sum_{j=1}^{I} \upsilon_j} - 1 \leq \xi_2; \ \forall i \in \{1, 2, ..., I\}$$

In this equation ζ_1 and ζ_2 are fairness limits and χi is the bitrate for subnet U_i.

A commonly used maximisation utility is the max-min algorithm-family, which states that a utility rate is min-max fair if and only if an increase of U_{tot} is distributed equally between the U_i's (Boudec, 2008). An algorithm that provides this is (Yaacoub, 2016), (14):

$$U(Rb) = -\sum_{i=1}^{I} \frac{1}{\alpha \cdot (v_i)^\alpha} \quad \alpha > 0 \qquad (14)$$

The α-parameter controls the degree of fairness. It is noted that this algorithm in addition to optimise fairness also minimises the total bit-rate $U(v)$. This means that power is saved in the WINs (they often run on batteries) and that a fair bit-rate is provided.

The proposed framework – a simulation model

A simulation model has been designed in Matlab (R2018a) to establish the performance of using BPSO to control interferences and at the same time provide fairness between the sub-networks. Without loss of generality, the model used in the simulations is a simplification of the previously discussed smart building model Figure 2 as shown in Figure 4.
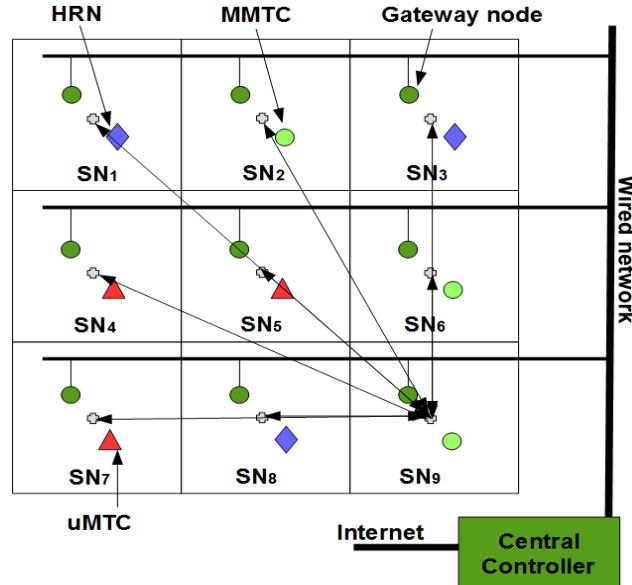

Figure 4, The simulation model with its node types (WINs) and the GWN connected to the central controller.

The model uses three different types of WINs to generalize its usability. Type 1 is a High Rate Node (HRN) which is assumed to transmit most of the time, i.e. it could be a camera-based user interface in an apartment. Type 2 is a Massive Machine Type Communication (MMTC) node which only transmits when activated, e.g. by a user that moves furniture in the apartment. Type 3 is an Ultra Reliable Machine Communication (uMTC) type which must have priority over the other nodes. An example application of this node type is important alarms, etc. The two last types are commonly known from the 5G evolution (Osseiran, 2014), (Yaacoub, 2016). In the process of simulating these node types the mask (9) needs to be deployed to sort and priorities the interferences. With regard to the MMTC nodes these only take the interferences from the HRNs into account by setting the M-mask appropriately. The reason is that the

MMTC nodes do not need instantaneous channel access, i.e. they commonly use a protocol that senses the channel state before transmitting (e.g. CSMA) and deploys a retransmission scheme which will back-off and retry if a collision occurs. Regarding the uMTC nodes these must always be able to get channel access, why all interferences are included by the mask (M-matrix-(9)). Similarly, the HRN must always be able to get channel access because these nodes need to continuously transmit data why the mask is set accordingly. In addition, the simulation model uses a distance matrix as indicated in Figure 4 (only paths for node SN-9 is shown) to find the path-loss matrix L (8).

No.	Simulation Parameters	
	Type	*Value*
1	Noise floor (Ng)	1.38e-23*300*1e6 [W]
2	Node bandwidth	1e6 [Hz]
3	Target BER for all nodes	<1e-3
4	Distance WIN to GWN inside a cluster	1.0 [m]
5	Distance between cluster centres	4.0 [m]
6	Binary mask matrix (M)	*HRN, MMTC ,uMTC provides interferences to HRN. *Only HRN provides interferences to MMTC and uMTC.
	Max transmit power	1e-3 [W]
8	BPSO: number of particles	100
9	BPSO: bits for Tx power level in sub-network SN$_x$	4 [bits]

Table 2, Parameters for the simulation model.

The following pseudo-code elaborates the working principles of the simulator code and how it uses the simulation parameters (Table 2) and the discussed equations (Figure 5).

```
1: Initialize all variables and define constants
2: Calculate L matrix
3: H=Mask L matrix with M matrix
4: p=0
5: X=default values // X is a tx power multiplier for SN1-9
6: Pcomp= default values  // measured SNR from GWNs
7: for p < P  // P is stop criterion
8:     X=BPSO(X,CF)
9: end for
10: CF function  // Cost function
11:     TxP=PSN*X   // eq(9)
12:     γ=LSN*TxP*Pcomp /(H*TxP+Ng)  // eq(7-11)
13:     ν =Bw*Se(γ) // eq(6-7)
14:     U(ν)=f(ν) // eq (13)
15:     return U(Rb)
16: end function
```

Figure 5, Pseudo-code for the flow of the simulation software including.

where: *X* parameter is a 4-bit transmit-power multiplier, γ is SNR, L_{SN} is path-loss from a WIN to its respective GWN, *Pcomp* is SNR from the GWN nodes, *L*-matrix is path-loss between the WINS multiplied with the mask matrix (*M*), *Ng* is additive white Gaussian noise from the channel. ν is the bit-rates.

As previously discussed, the novelty of this work is regulating the fairness of the bit-rates for all nodes as a function of transmit-power by using a centralized controller equipped with a nonlinear BPSO optimization algorithm. By deploying this system significant power savings can be achieved, impact of interferences can be reduced, and spectrum utilization can be lowered relative to a greedy-based scenario. This optimization process takes place in the central controller, where each optimization step is presented as pseudo-code in Figure 5.The main functionality takes place in lines 7 to 9, where the BPSO algorithm is called with the parameters X and CF. The X parameter is a trial vector used by the BPSO algorithm to find the optimal transmit-powers given the parameters in Table 2, and the CF parameter is the cost function given in lines 10 to 15. In a real setting the cost function receives the SNR (γ) from all the nodes; however, in a simulator environment the node SNRs need to be calculated - this takes place in line 11 and 12. The received SNR is used by the cost function (line 13) to find the bit-rates for all nodes given the conditions in Table 2. Based on the bit-rates the cost function calculates and return the cost in line 14 and 15. Hence, by looping the BPSO with the cost function as parameter the transmit-power that optimises the fairness of bit-rates will be found and returned to the WINs.

Simulation results

In the following section the results from the simulations performed by the model discussed in the previous section is presented and elaborated.

Simulation outcomes

To be able to elaborate the principles and the algorithms the path-loss in the first three runs of the simulated model is fixed to 1e-6 for all sub-networks (SNs). From the simulated results it is observed that the spreading of the bit-rates between the WINS is low. This is caused by the central controller which optimises the bit-rates given the condition that the path-losses are all equal.
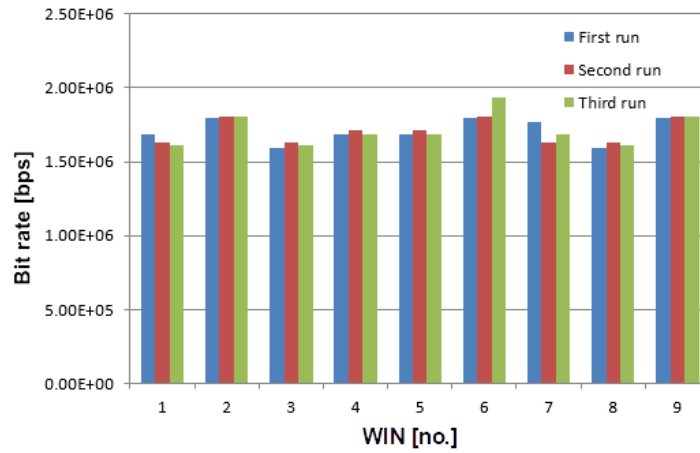

Figure 6, Simulated bit-rates for a fixed path-loss (1e-6) where the three columns are different runs with the same parameters.

As discussed, the uMTC and HRN nodes needs to coexist why they share the same spectrum by using Space Division Multiple Access (SDMA), i.e. no masking takes place in the simulator. As regards the MMTC nodes they use access control schemes like CSMA, i.e. they back-off if the channel is busy. The channel is considered busy if and only if one or more uMTC nodes transmits, whereas the HRN nodes are considered as noise (their interferences are added to the noise part of the node SNR). Hence, the interferences from the HRN nodes are included the tx power allocation for the MMTC nodes. This means that the uMTC and the MMTC nodes share the same channel capacity, i.e. their effective bit-rates in

Figure 6 cannot co-exist. The reason for this masking process is that the uMTC nodes in most smart building scenarios are allocated to short messages such as alarms and other important control information which needs a very short delay (Lynggaard & Skouby, 2015). However, these messages are not sent on a regular basis, i.e. they only use the available bit-rate for a very short time-period. Hence, the interferences produced by the uMTC nodes are masked out by the MMTC nodes. It is noted that this masking only works one way (from the uMTC to the MMTC), i.e. the uMTC devices can sense all interferences in the system. This is a necessary condition to ensure that these devices can send at any time. On the other hand, the MMTC devices are often allocated to sense events in its context such as movement sensors, temperature sensors, and different types of binary sensors. These types of events can be delayed without loss of contextual and temporal information (Lynggaard & Skouby, 2015).
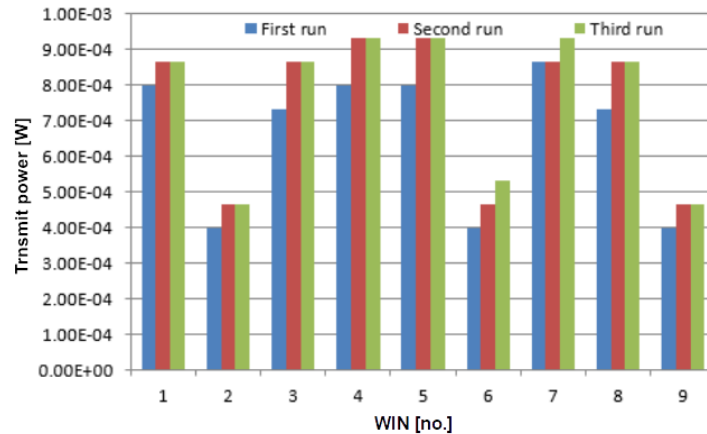

Figure 7, Simulated transmit-powers for a fixed path-loss (1e-6). The three bars are three different runs with the same parameters.

Figure 7 shows the amount of transmit-power needed by the WINs to achieve the bit-rates presented in Figure 6. It is observed that WINs 2, 6, and 9 (the MMTC nodes) use approximately 50 percent less transmit-power than the other WINs. This is a result of the used mask (*M* matrix) in the model-runs, because it forces the MMTC nodes to ignore the interference levels as stated previously. Hence, these nodes sense a reduced interference level where it is assumed that the uMTC nodes do not transmit. This means that in order to overcome the sensed interference level need less power compared to the other devices which sense the full interference level.
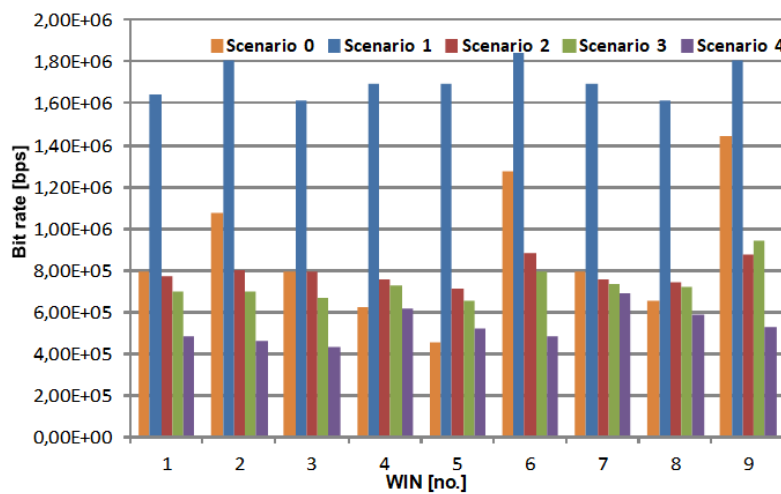

Figure 8, Simulated bitrates as a function of node numbers and usage scenarios.

The results of model-runs with: greedy settings (scenario 0), fixed path-loss settings (scenario 1), full model (scenario 2), full scenario with 6 dB extra path-loss for node 3 (scenario 3), and full scenario with

10 dB extra path-loss for node 3 (scenario 4) are presented in Figure 8 and Figure 9 respectively. Regarding the greedy scenario (scenario 0) it is noted that the bit-rates fluctuate significantly more than the regulated cases (scenario 1-4), i.e. its minimum and maximum values deviates from the average value with +48 and -64 percent. This should be compared to the full model (scenario 2) which deviate between +10 and -12 percent. Furthermore, it is noted that the effective bit-rate for the fixed path-loss model (scenario 1) provides approximately the double bit-rate compared to the other models. This is expected because the path-loss is smaller in this model. In addition, it is noted that the extra path-loss added to node 3 (scenarios 3 and 4) is equalized by the central controller. The 10 dB extra loss (scenario 4) means the controller needs to lower the transmit-power for all the nodes, why the averaged bit-rate drops for all nodes.
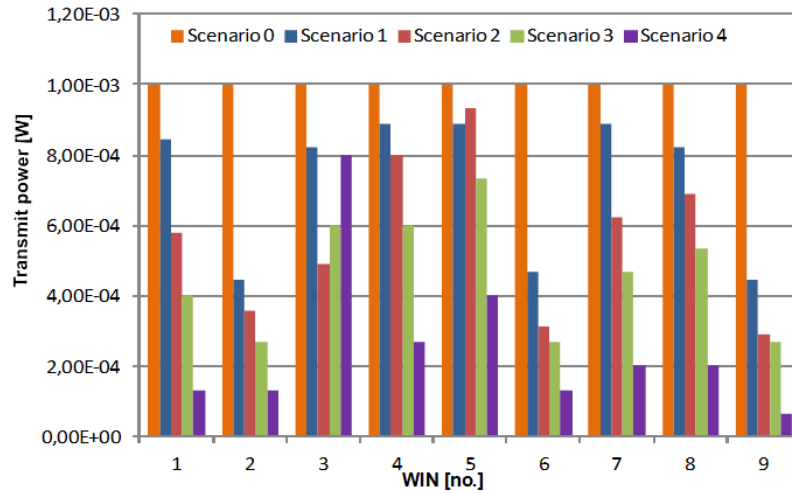

Figure 9, Simulated transmit-powers as a function of node numbers and usage scenarios.

From Figure 9 it is noted that the highest transmit-power is found in the greedy scenario (scenario 0) where all nodes use the maximum transmit-power. The second highest transmit-power consumption is the scenario with fixed path-loss (scenario 1). As elaborated, this is caused by the path-loss being the smallest and by the masking of some nodes. In scenario 3 and 4 it is observed that the attenuation imposed on node 3 forces the WINs to increase their transmit-powers to compensate for this. However, this increase in transmit-powers changes the interference patterns for all the nodes why the central controller re-calculates the average transmit-power in the system.

The transmit-power used by the WINS is directly proportional to their consumed (battery) power, why reducing this would save approximately the same amount of power (Lynggaard & Skouby, 2015). For scenario 1 to 4 the average transmit-powers are: 7e-4, 5e-4, 4e-4, 2e-4 W. By comparing these numbers to the numbers without this protocol, i.e. a greedy scenario (scenario 0) where all nodes use maximum power (1e-3 W each), the significance of this technique is presented, i.e. the savings are in the range of 28 to 74 percent.

The bit-rate performance and the transmit-power performance in terms of changing the BER for the receivers (scenario 2) from 10^{-3} to 10^{-5} are presented in Figure 10 and Figure 11 respectively.
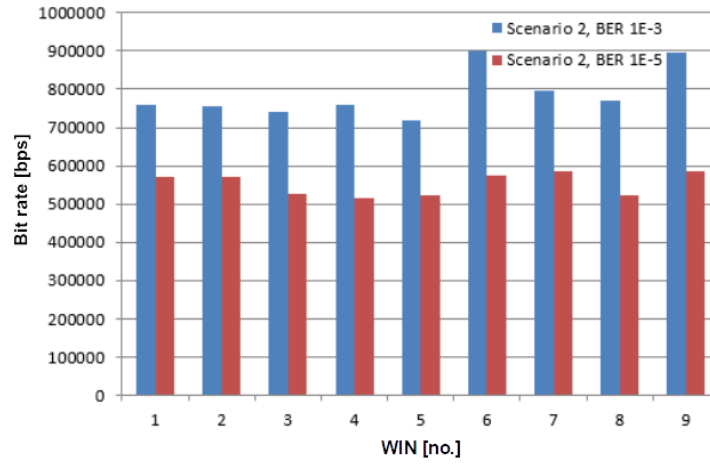
From Figure 10 it is noted that when the required BER for the receiving nodes is increased (from 10^{-3} to 10^{-5}) the central controller lowers the bit-rates and the transmit-powers (Figure 11) for all the WINS. This is the case because lowering the bit-rates increase the energy-per-bit divided by noise-spectral-density (Eb/N0) to the level required by the given BER. In addition, lowering the transmit-power reduces the summed interference power from all the nodes. Hence, the central controller ensures that allocated transmit-powers for all WINS are regulated so the total channel capacity is divided in a fair way. In case a node is close to its sensitivity limit the central controller will gracefully degrade its QoS in the form of degrading its bit-rate. Similarly, if the load conditions vary over time one or more of the WINS will detect this in the form of a changing SNR and afterwards send a message to the central controller. The central controller then recalculates power allocations for all the WINS.
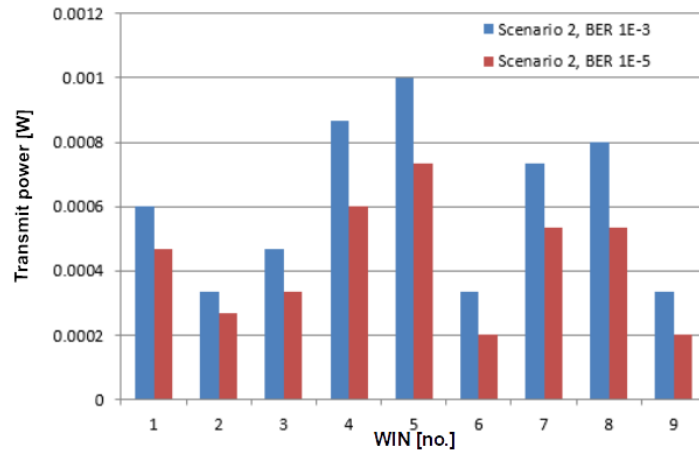
Focusing on the convergence performance (y-axis) of the BPSO algorithm it is presented in Figure 12 where the two curves show the "fixed path-loss" and the "full model" as a function of the number of iterations.
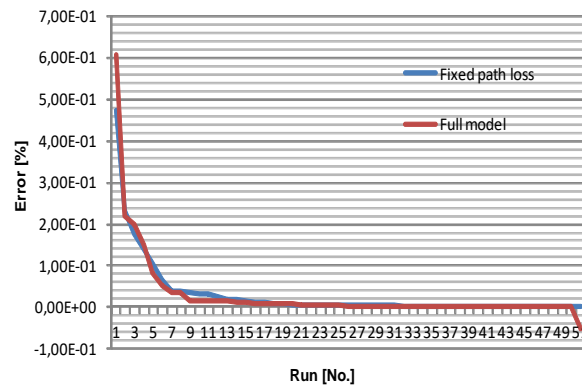
Figure 12, The convergence-rate of the BPSO algorithm.

As illustrated in Figure 12 the algorithm converges after approximately 25 iterations. It is noted that even though the calculation complexity grows considerably in the full model compared to the fixed path-loss model the BPSO convergence rates are almost similar. This is caused by the optimisation process implicitly implemented in the BPSO algorithm. This process randomly moves the correlated particles in the direction of the optimum without using complexity dependent elements such as the least mean square algorithm would do in the form of a gradient vector.

To establish some quantitative efficiency measures and to substantiate the performance results of the proposed system it is compared to similar state-of-the-art systems in terms of performance (Table 3). From the comparison it is noted that the proposed system is comparable with similar systems in terms of package-receiver-ration and that it offers a very good performance with respect to battery power savings.

Number:	Project:	Package Receive Ratio (PRR)	Battery power savings
1	This work (scenario 4)	95%	74%
2	ART (Chincoli & Liotta, 2018)	94%	NP
3	SVM method (Popovski, 2014)	84-89%	NP
4	Reinforcement learning method (Lu, et al., 2018)	95%	52%
5	PECC-algoritme (PSO) (Vimalarani, et al., 2015)	95%	53%

NP means that the data is not provided by the author. Data in reference 2 and 5 have been estimated from figures in the papers.

Table 3, peformance comparison with similar systems

Conclusion

The current research efforts in centralized IoT device-control to reduce the impact of interferences, reduce transmit-powers, and reduce spectrum utilizations are oriented towards the deployment of machine learning. Machine learning algorithms are able to regulate the behaviour of IoT devices in a global context by deploying nonlinear cost functions. One such machine learning algorithm is the BPSO algorithm. It has some interesting properties, because it is able to optimize nonlinear cost functions; it is meta-heuristics, i.e. it does not make a lot of assumptions about the problem being solved; and it is able to deal with discrete variables which are commonly used in transmit-power control schemes for IoT nodes. In this paper a simulation model for a centralized controller concept based on a nonlinear cost function has been derived to substantiate the potential of this concept. This model simulates how a BPSO based centralized controller can handle the co-existence of IoT sub-networks to reduce interferences, save power and dynamically adapt to network changes. It has been found that the proposed algorithm

effectively solves a nonlinear cost function (less than 25 iterations) and that it produces a fair bit-rate allocation with a deviation from the average value with +/- 10 and 12 percent compared to a greedy case (no controller regulation) where the deviations from the average value are +/- 48 and 64 percent. In addition, the controller regulation saves between 28 and 74 percent transmit-power compared to a greedy case. These considerable savings in transmit-powers mean that interference levels decrease with similar percentages.

The potential of deploying the presented system in future smart buildings is very large because it is able to regulate the transmit-powers as a function of the pathlosses and Rayleigh fading. By reducing the transmit-powers the interference levels are lowered proportionally which means that IoT devices in different apartments can coexist within the same building. In addition, the presented concept is able to offer selective bit-rates for the different node types meaning that different types of services with different QoS needs can coexist. Another significant outcome is the simulations results of the deployed nonconvex optimization algorithm (BPSO algorithm) which shows that this algorithm is very efficient in the context of optimising nonconvex cost functions in relation to constructing a services framework for smart buildings.

References

Abdellaoui, S., Debbah, M., Fakhri, Y. & Aboutajdine, D., 2013. Increasing Network Lifetime in an Energy-Constrained Wireless Sensor Network. *International Journal of Sensor Networks.*

Auger†, A. et al., 2009. *Experimental Comparisons of Derivative Free Optimization Algorithms.* s.l., International Symposium on Experimental Algorithms.

Boudec, L., 2008. *Rate adaptation, congestion control and fairness: a tutorial. ,* s.l.: s.n.

Chincoli, M. & Liotta, A., 2018. Self-Learning Power Control in Wireless Sensor Networks. *Sensors.*

Chincoli, M., Syed, A., Exarchakos, G. & Liotta, A., 2016. Power Control in Wireless Sensor Networks with Variable Interference. *Mobile Information Systems.*

Chung, S. & Goldsmith, A., 2001. Degrees of freedom in adaptive modulation: a unified view. *IEEE Trans Wireless Communication.*

Falahati, S., Svensson, A., Sternad, M. & Ekman, T., 2003. *Adaptive Modulation Systems for Predicted Wireless Channels.* s.l., s.n.

Fré, G., Reis, F., Silva, J. & Mendes, L., 2015. Particle Swarm Optimization Implementation for Minimal Transmission Power Providing a Fully Connected Cluster for the Internet of Things. *International Workshop on Telecommunications (IWT) .*

Gharghan, S., Nordin, R., Ismail, M. & Ali, J., 2016. Accurate Wireless Sensor Localization Technique Based on Hybrid PSO-ANN Algorithm for Indoor and Outdoor Track Cycling. *IEEE sensors journal.*

Gogu, A., Nace, D., Chatterjea, S. & Dilo, A., 2014. central control of interference in wsn. *Journal of Applied Mathematics;.*

ITU, 2001. *ITU Model for Indoor Attenuation,* s.l.: s.n.

ITU, 2018. [Online] Available at: https://www.itu.int/en/publications/Pages/default.aspx

Kennedy, J. & Eberhart, R., 1997. A discrete binary version of the particle swarm algorithm. *Systems, Man, and Cybernetics.*

Kinhekar, N. & Gupta, H., 2015. Particle Swarm Optimization Based Demand Response for Residential Consumers. *IEEE Power & Energy Society General Meeting.*

Kuila, P. & Jana, P., 2014. A novel differential evolution based clustering algorithm for wireless sensor networks. *Applied Soft Computing.*

Kulkarni, R. & Venayagamoorthy, G., 2011. Particle Swarm Optimization in Wireless Sensor Networks: A Brief Survey. *IEEE Transactions on system, man, and cybernetics-part c:applications and reviews.*

Kumar, S., Gupta, P., Singh, G. & Chauhan, D., 2013. Performance Analysis of Rayleigh and Rician Fading Channel Models using Matlab Simulation. *I.J. Intelligent Systems and Applications,* Volume 9.

Lu, B. et al., 2018. A Dynamic SelfAdapting Mechanism for ZigBee Performance Assurance Under Wi-Fi Interference. *IEEE Sensors Journal.*

Lynggaard, P. & Skouby, K., 2015. Complex IoT Systems as Enablers for Smart Homes in a Smart City Vision. *Sensors*.

Lynggaard, P. & Skouby, K., 2015. Deploying 5G-technologies in smart city and smart home wireless sensor networks with interferences. *Wireless Personal Communications.*

Muhammad, I. et al., 2015. Wireless Sensor Network Optimization Multi-Objective Paradigm. *Sensors.*

Nandi, A. & Kundu, S., 2010. Evaluation of Optimal Transmit Power in Wireless Sensor Networks in Precense of Rayleigh Fading. *Journal of Communication Technology.*

Osseiran, A., 2014. 5G beyond the hype. *Ericsson Business Review*, Volume 2.

Pathak, S. & Katiyar, H., 2016. Performance Analysis of Wireless link in Rician Fading Channel. *International Journal of Advanced Research in Computer and Communication Engineering,* Volume 5.

Popovski, P., 2014. Ultra-Reliable Communication in 5G Wireless Systems. *International Conference on 5G for Ubiquitous Connectivity (5GU).*

Qiu, X. & Chawla, K., 1999. On the Performance of Adaptive Modulation in Cellular Systems. *IEEE Transactions on communications.*

Shi, Y. & Eberhart, R., 1999. Empirical Study of Particle Swarm Optimization. *Evolutionary Computation.*

Sklar, B., 2002. *Digital communications, fundamentals and applications.* Second edition ed. s.l.:Pearson.

Vimalarani, C., Subramanian, R. & Sivanandam, S., 2015. An Enhanced PSO-Based Clustering Energy Optimization Algorithm for Wireless Sensor Network. *The Scientific World Journal.*

Wang, C., Sun, E. & Tian, F., 2016. Optimal Coverage Algorithm of Wireless Sensor Networks Based on Particle Swarm Optimization with Coherent Velocity. *International Journal of Grid and Distributed Computing.*

Weng, C., Zhang, J. & Hung, H., 2014. An efficient power control scheme and joint adaptive modulation for wireless sensor networks. *Computers and Electrical Engineering.*

Yaacoub, E., 2016. *Green 5G Femtocells for Supporting Indoor Generated IoT Traffic.* s.l.:Springer.

ZHOU, Y., WANG, N. & XIANG, W., 2017. Clustering Hierarchy Protocol in Wireless Sensor Networks Using an Improved PSO Algorithm. *IEEE Access.*